Bulletin of the Seismological Society of America, 92, 1, pp. 322–329, February 2002

Lithospheric Structure of the Marmara and Aegean Regions, Western Turkey

by Gündüz Horasan, Levent Gülen, Ali Pınar,* Doğan Kalafat, Nurcan Özel, H. Sadi Kuleli, and A. M. Işıkara

Abstract We have simulated the waveforms of three aftershocks of the İzmit (17 August 1999) earthquake, with magnitudes greater than *M* 5.0, to determine the lithospheric structure of the Gulf of İzmit, Marmara region. Using the discrete wavenumber technique (Bouchon, 1981), different layered crustal models have been tested for the simulation of the waveforms, and the best crustal model was determined by a best-fit criterion between the observed and simulated seismograms. Our results indicate that the average thickness of the crust is 32 km and that *Pn* and *S* velocities are 8.0 and 4.60 km/sec, respectively, in the Gulf of İzmit, Marmara region.

We also computed synthetic waveforms of the 21 April 2000 Denizli (Honaz) and the 9 July 1998 İzmir (Doğanbey) earthquakes in the Aegean in order to compare the lithospheric structures of the Marmara and the Aegean regions. The Aegean region has an average crustal thickness of 33 km and *Pn* and *S* velocities of 7.85 and 4.53 km/sec, respectively. Although thicknesses of the crusts are comparable and suggest an approximately equal amount of E–W stretching in the Marmara and N–S stretching in the Aegean regions, a patchy midcrustal low-velocity zone exists in the Aegean.

The upper-mantle *Pn* velocity variation between the Marmara and the Aegean regions is interpreted as the effect of a thinning continental lithosphere toward the active Aegean arc and the establishment of a consequent upper-mantle temperature gradient, increasing from the north to the south. Additionally, the Black Sea oceanic lithosphere that steeply dips southward beneath the Marmara region, as evidenced by the seismic tomographic results obtained by Gülen and Kuleli (1995), can contribute to the advective cooling of the upper mantle that causes relatively high *Pn* velocities in the Marmara region.

Introduction

The active tectonics of the Marmara and the Aegean regions of western Turkey are mainly dominated by the right-lateral strike-slip North Anatolian Fault (NAF) in the north and the active Aegean subduction along the Hellenic Trench in the south, respectively (Fig. 1). Whereas approximately E–W extension, related to the dextral strike-slip NAF, is taking place and is mainly responsible for the formation of an enormous, complex pull-apart Marmara Sea basin in the north, a N–S extension takes place within the back arc type extensional tectonic regime in the Aegean region to the south.

The NAF is a well-known seismically active strike-slip fault that extends for about 1500 km from the Karliova Junction in eastern Turkey to Greece (Ketin, 1969; Ambraseys, 1970; Şengör, 1979; Barka and Gülen, 1988; Barka, 1992). The NAF forms the tectonic boundary between the Anatolian and the Eurasian Plates, and it accommodates the westward motion and counterclockwise rotation of the Anatolian Plate relative to the Eurasian Plate (McKenzie, 1972; Dewey and Sengör, 1979; McClusky *et al.,* 2000; Gülen *et al.,* 2002). The NAF splays into three strands to the west of the Mudurnu Valley (31.5° E) in the Marmara region (Barka and Kadinsky-Cade, 1988). The 17 August 1999 İzmit earthquake occurred along the northern strand of the NAF (Gülen *et al.,* 2002). The Marmara Sea pull-apart basin was formed apparently because of a total displacement of 85 km along these three strands over the past 5 m.y., which caused significant stretching of the continental crust in the Marmara region (Armijo *et al.,* 1999). Global Positioning System measurements indicate an even higher amount of recent slip

*Present address: Department of Geophysical Engineering, Istanbul University, 34850 Avcılar, Istanbul, Turkey.

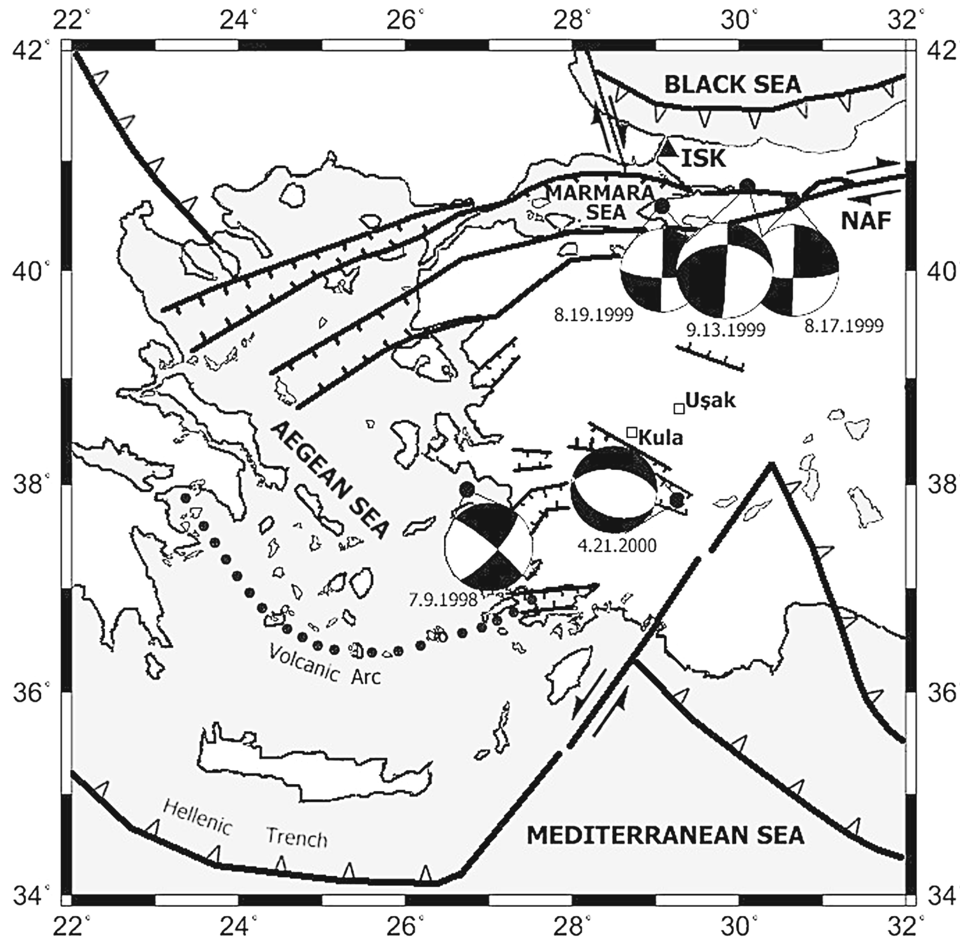

Figure 1. Simplified tectonic map of the Marmara and the Aegean regions (after Gülen *et al.,* 2002). The earthquake epicenters, focal mechanism solutions, and the location of the broadband station Istanbul Kandilli (ISK) are also shown. Compressional regions are black in the focal spheres.

rates (total 22 ± 3 mm/yr) along these three strands (Straub *et al.,* 1997).

The Aegean continental lithosphere overthrusts the Mediterranean oceanic lithosphere along the Hellenic Trench, forming the active Aegean subduction zone to the south. The active Aegean volcanic arc, which consists mostly of small volcanic islands, stretches between Greece and Turkey. Extension-related alkali volcanics, such as the Kula basalts and older Oligocene to Miocene calc-alkaline volcanics cover extensive areas (Fytikas *et al.,* 1984; Gülen, 1990). The Aegean region is dominated by an extensional tectonic regime, as evidenced by numerous E–W-trending normal faults, high seismic activity, and extensional earthquake focal mechanisms (Alptekin, 1973; McKenzie, 1978; Dewey and Şengör, 1979; Taymaz *et al.,* 1991). Crustal thicknesses of 30 km in Kula and 34 km in Uşak were determined using teleseismic receiver functions, and comparison of these with the presumably unstretched crustal thickness of 38 km in Ankara implies an extensional β-factor of about 1.2 for the Aegean region (Saunders *et al.,* 1998). This estimate is close to 1.3, determined by the integration of seismic strain rates in western Turkey (Eyidoğan, 1988).

Our goal in this study is to investigate the lithospheric structure of the Gulf of İzmit, Marmara region, and compare it with that of the Aegean.

Data Processing and Waveform Modeling

The data used in this study were obtained from the Boğaziçi University, Kandilli Observatory and Earthquake Research Institute database. The recording system is a broadband high dynamic range instrument, installed at station ISK (Istanbul-Kandilli). The observed broadband data have been integrated to ground displacement and converted into radial and transversal components.

We synthesized the waveforms using the discrete wavenumber technique (Bouchon, 1981). This technique allows the synthesis of seismograms, including all body and surface waves. We have tried different layered crustal models for the synthetic seismograms and compared them with the observed ones. The best model inferred by the best fit between observed and synthetic waveforms, is evaluated by the correlation coefficients.

Waveforms from three major aftershocks (17 August 1999 $M_b = 5.3$; 19 August 1999 $M_d = 5.0$; 13 September 1999 $M_b = 5.8$) are investigated. The locations of the earthquake epicenters are given in Figure 1 and Table 1. The displacement records that we use are shown in Figures 2–4. We did not calculate the radial component of the 13 September 1999 earthquake in Figure 4 because source and propagation parameters for the computation of the synthetic seismograms were unavailable. We used time windows of 100 and 75 sec and frequencies up to 1 Hz for the calculations. All synthetic seismograms consist of 225 points. We obtained a good agreement between the observed and the synthetic seismograms at the ISK broadband station with a rise time t_0 of 3 sec. Simulated and observed waveforms at the ISK station are shown in Figures 2–4.

First, we held the source parameters (location, depth, and focal mechanism) fixed, and then we changed the velocity model parameters. After the source parameters were constrained, the velocity model was perturbed until a good

Table 1
Epicentral Data and Fault-Plane Solutions for the 1999 Izmit Earthquake Aftershocks

Date (dd/mm/yy)	Origin Time (UTC)	Latitude (°N)	Longitude (°E)	Magnitude (*M*)	Focal Mechanism*	Reference
17/08/1999	03h14m20sec	40.64	30.65	5.3	91 76 179	USGS, 1999
19/08/1999	15h17m00sec	40.59	29.08	5.0	91 76 179	USGS, 1999
13/09/1999	11h15m00sec	40.77	30.10	5.8	270 46 176	USGS, 1999
21/04/2000	12h23m10sec	37.85	29.26	5.2	113 39 77	USGS, 2000
9/07/1998	17h36m47sec	37.95	26.74	5.3	42 75 172	Türkelli *et al.* 1995

*Strike, dip, and rake (ϕ, δ, γ).

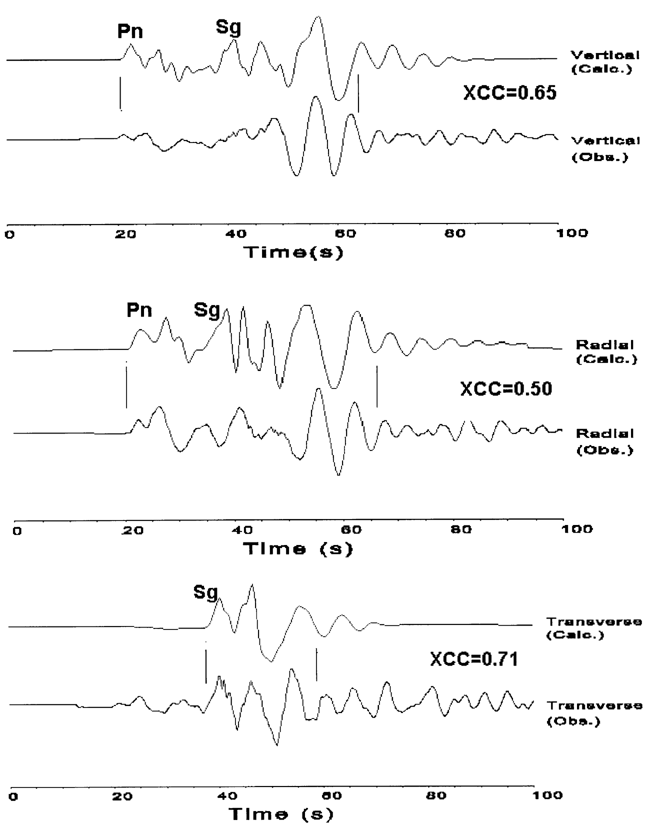

Figure 2. Comparison of the three-component (vertical, radial, and tangential) calculated (first trace) and recorded (second trace) synthetic displacement seismograms at ISK for the 17 August 1999 İzmit earthquake aftershock. Traces are low-pass filtered at 1.0 Hz.

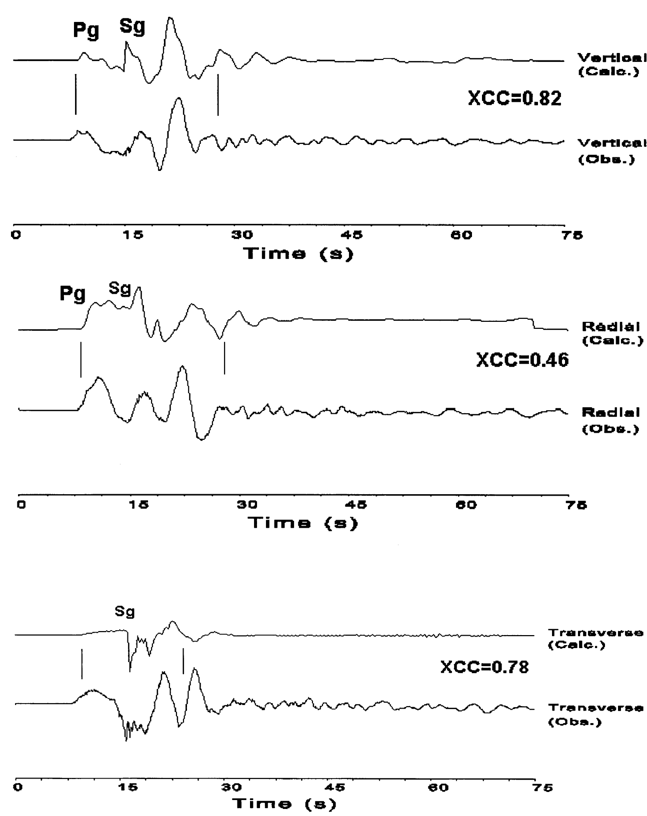

Figure 3. Comparison of the three-component (vertical, radial, and tangential) calculated (first trace) and recorded (second trace) synthetic displacement seismograms at ISK for the 19 August 1999 İzmit earthquake aftershock. Traces are low-pass filtered at 1.0 Hz.

agreement with the data was obtained. A fitting criterion (cross-correlation coefficient—XCC) is applied to the observed and simulated seismograms in the selection of the best model. For the best model, the XCCs between the observed and synthetic waveforms for the three aftershocks are shown in Figures 2–4. These coefficients range from 0.46 to 0.82 for all the components. We used a time window to calculate the correlation coefficients, neglecting the *S*-phase coda. The radial component correlation coefficient of the earthquakes is lower than for the other components. The generally low correlation coefficients of the radial components may indicate lateral variation in the thicknesses or velocities of the layers. The velocity model parameters for three aftershocks are given in Table 2. The crust is 32 km thick, and the upper-mantle *Pn* and *Sn* velocities are 8.0 and 4.6 km/sec, respectively, in the Gulf of İzmit, Marmara region (Table 2 and Fig. 7a). The crustal phases are well seen and are marked on the seismograms. The phases on the synthetic seismograms are identified from the travel-time curves using a ray-tracing program.

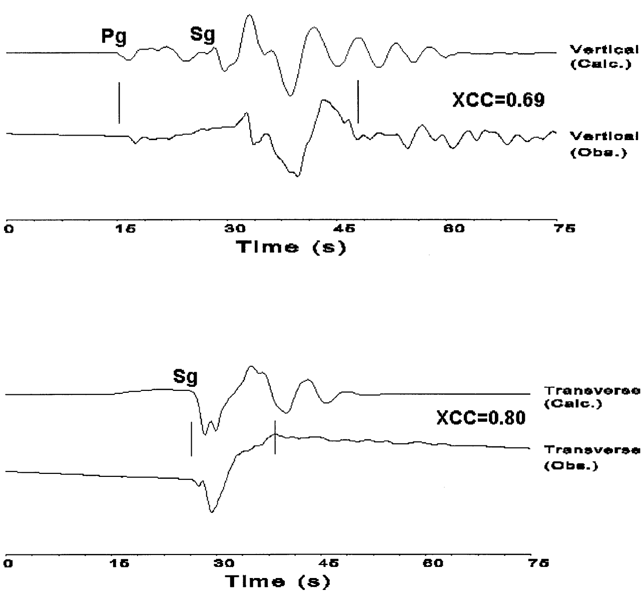

Figure 4. Comparison of the two-component (vertical and tangential) calculated (first trace) and recorded (second trace) synthetic displacement seismograms at ISK for the 13 September 1999 İzmit earthquake aftershock. Traces are low-pass filtered at 1.0 Hz.

Table 2
Crust and the Upper Mantle Model for the Gulf of Izmit, Marmara Region Determined from the İzmir Earthquake Aftershocks

Thickness (km)	V_p (km/sec)	V_s (km/sec)	Density (g/cm^3)	Q_P	Q_S
04	3.50	2.20	2.00	300	150
13	5.80	3.40	2.70	300	150
15	6.20	3.60	2.80	400	200
	8.00	4.60	3.34	1000	500

We also modeled the 21 April 2000 Denizli (Honaz) earthquake (M_d 5.2) and the 9 July 1998 İzmir (Doğanbey) earthquake (M_b 5.3), in order to determine the crustal and the upper-mantle structure of the Aegean region. The epicenters of these earthquakes are located at 37.85° N, 29.26° E and 37.95° N, 26.74° E, respectively. These two earthquakes were recorded digitally at regional distance by the ISK broadband station.

We used approximate source parameter values for the Denizli (Honaz) earthquake by assuming that the mechanism is similar to that of the 24 February 1989 Denizli earthquake (M_b 5.0) that occurred in the same region (37.73° N and 29.34° E; strike 113°, dip = 39°; slip = 77°) (U.S. Geological Survey [USGS] earthquake database). The fault mechanism solution is taken from the studies of Türkelli *et al.* (1995) (strike 42°; dip 75°; slip = 172°) for the İzmir (Doğanbey) earthquake. Simulated and observed waveforms at the ISK station are shown in Figures 5 and 6. The correlation coefficients range from 0.44 to 0.80 for the components. All correlation coefficients are greater than 0.50, except for the vertical component of the 9 July 1998 earthquake. The crust

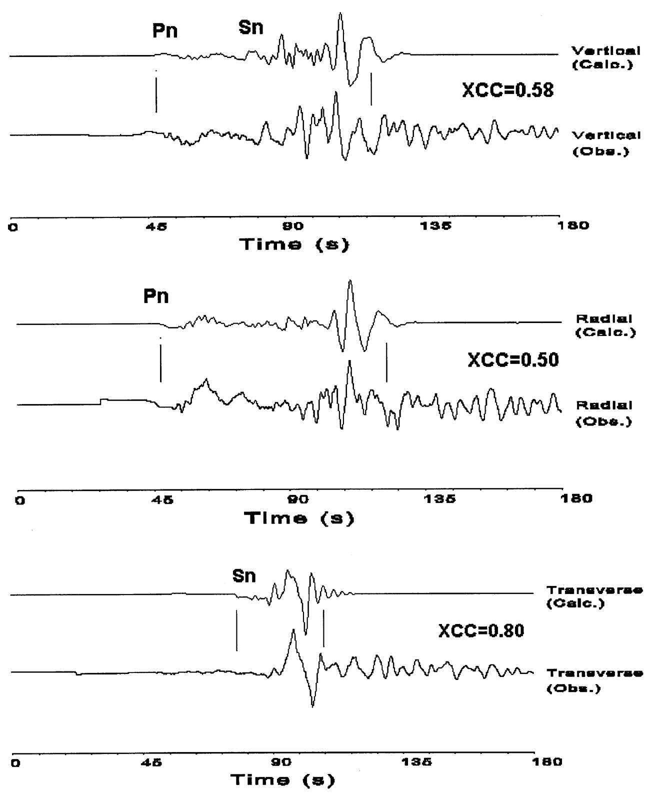

Figure 5. Comparison of the three-component (vertical, radial, and tangential) calculated (first trace) and recorded (second trace) synthetic displacement seismograms at ISK for the 21 April 2000 Denizli (Honaz) earthquake. Traces are low-pass filtered at 1.0 Hz.

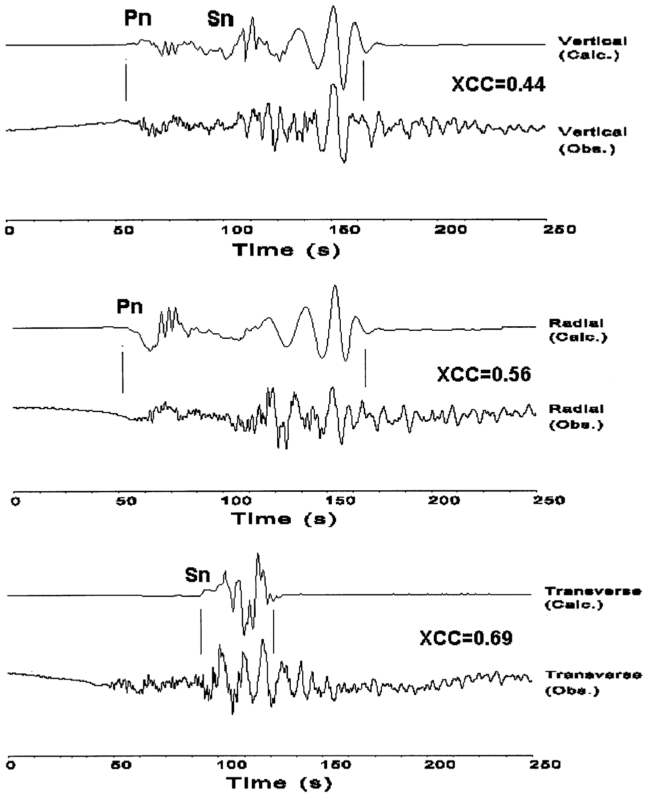

Figure 6. Comparison of the three-component (vertical, radial, and tangential) calculated (first trace) and recorded (second trace) synthetic displacement seismograms at ISK for the 9 July 2000 İzmir (Doğanbey) earthquake. Traces are low-pass filtered at 1.0 Hz.

Table 3
Crust and the Upper Mantle Model for the Aegean Region Determined from the 21 April 2000 Denizli (Honaz) and 9 July 1998 İzmir (Doğanbey) Earthquakes

Thickness (km)	V_p (km/sec)	V_s (km/sec)	Density (g/cm^3)	Q_P	Q_S
02	4.50	2.60	2.00	100	80
08	5.80	3.35	2.50	200	100
05	5.50	3.20	2.35	190	95
18	6.10	3.87	2.80	350	175
	7.85	4.53	3.10	1000	500

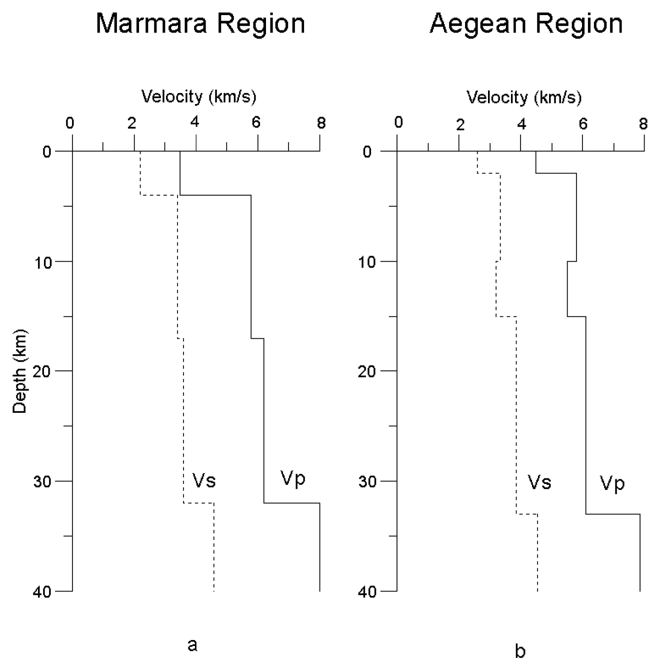

Figure 7. *P* and *S*-wave crustal velocity models for (a) the Gulf of İzmit, Marmara region and (b) the Aegean region.

is 33 km thick, and the upper-mantle *Pn* and *Sn* velocities are 7.85 and 4.53 km/sec, respectively, in the Aegean region (Table 3 and Fig. 7b).

Discussion

The velocity structure of the crust and upper mantle in this area has been studied using travel times from local earthquakes (Crampin and Üçer, 1975; Gürbüz *et al.,* 1992), quarry blasts (Gürbüz, 1980), and seismic tomography studies (Kuleli, 1992; Gülen and Kuleli, 1995). Earthquake and quarry blast experiments indicate *Pn* velocity values (8.0 km/sec) in the Marmara region. The average *Pn* velocity for the entire Aegean region is approximately 7.9 km/sec (Panagiotopoulos and Papazachos, 1985), which is lower than the worldwide average continental upper-mantle *Pn* velocity of 8.1 km/sec (Mooney and Braile, 1989).

In previous studies investigating the crustal structure, time—distance graphics composed of travel times of wave phases from different distances were analyzed, and crustal structures that yield these travel times were obtained. Layered structure of the crust not only affects the travel times of the seismic waves, but also the waveforms. Because waveforms are also calculated in addition to travel times in this study, the construction of synthetic seismograms allows maximum information to be obtained.

Based on our best model, we obtained an average crustal thickness of 32 km and *Pg* and *Pn* velocities of 5.9 and 8.0 km/sec, respectively, in the Gulf of İzmit, Marmara region.

We obtained a crustal thickness of 33 km and upper-mantle *Pn* and *S* velocities of 7.85 and 4.53 km/sec, respectively, for the Aegean region (Fig. 7b). A midcrustal low-velocity zone also exists within the crust at a depth of 10–15 km in the Aegean region. These results are consistent with our earlier studies (Horasan *et al.,* 1996) that suggest the presence of a patchy low-velocity layer within the crust in this region. Using teleseismic receiver functions, Saunders *et al.* (1998) corroborated our results.

Because our modeling accounts for the layered crustal structure, the observed *Pn* velocity variations in western

Turkey can be attributed to the lateral variations in the upper-mantle structure beneath this region. The existence of significant lateral variations in the upper-mantle structure is indicated by the reported *Pn* velocities ranging from 8.2 to 7.6 km/sec from the Black Sea to the Mediterranean Sea (Spakman *et al.,* 1988; Ligdas *et al.,* 1990; Kalafat *et al.,* 1992; Kuleli, 1992; Hearn and Ni, 1994; Papazachos *et al.,* 1995). The significant range observed in the *Pn* velocities reflects lateral variations in the thermal state and compositional nature of the upper mantle in western Turkey.

Based on a detailed study of *Pn* velocity and heat flow data in north America, Black and Braile (1982) found a statistically significant inverse relationship between *Pn* velocity and heat flow data and concluded that the variation in *Pn* velocity is primarily a temperature effect. Murase and Kushiro (1979) and Murase and Fukuyama (1980) experimentally demonstrated that the compressional-wave velocity of a typical upper-mantle rock, spinel-lherzolite at 10 kbar, under dry conditions, decreases from 7.8 km/sec at 1000°C to 7.4 km/sec at 1225°C and drastically decreases to 7.0 km/sec at 1270°C, when the amount of partial melt is about 3% by volume. Because only a few percent partial melt has such a profound lowering effect on the *Pn* velocities, we can expect the presence of a partially melted upper-mantle zone beneath the active Aegean volcanic arc and above the subducting slab, where the *Pn* velocities reach their lowest values around 7.6 km/sec. Active arc volcanism, measured high-heat values reaching up to 2.73 heat flow units (Erickson *et al.,* 1977; Fytikas and Kolios, 1979), and the presence of a zone of high *S*-wave attenuation (Kovachev *et al.,* 1991; Taymaz, 1996; Gök *et al.,* 2000) support this conclusion.

Identification of a partially melted upper-mantle zone does not necessarily indicate upper-mantle temperatures that are in excess of or at the dry spinel-lherzolite solidus because the aforementioned experiments may not truly represent the upper-mantle compositions in a subduction setting. The melting temperature (solidus) is a function of composition as well as pressure. If the mantle wedge above the subducting slab is fluxed by volatiles such as H_2O and CO_2 through the dehydration of the slab, this has an effect of lowering the dry solidus by about 200°C, depending on the degree of saturation. Upper-mantle xenoliths brought up by the lavas of Kula basalts in western Turkey contain hydrous phases, such as kaersutite, apatite, phlogopite, and sphene, in addition to olivine and clinopyroxene, indicating modal metasomatism and the existence of at least undersaturated hydrous conditions in the Aegean upper mantle (Gülen, 1990).

The solidus of the upper-mantle peridotites also decreases markedly with decreasing Mg number: Mg/(Mg + åFe) (Mysen and Boettcher, 1975). The Mg number may vary significantly depending on the degree of depletion or metasomatic enrichment of the upper mantle.

Because *Pn* velocity variations are more precisely a function of homologous temperature, the ratio of temperature to solidus temperature (Sato *et al.,* 1989), and because the partial melt fraction is also dependent on the homologous temperature, we cannot neglect the mantle composition effect on the *Pn* velocity variations. The upper-mantle temperature estimates based on the experiments discussed previously, which were carried out using high frequencies (100–800 kHz), cannot be realistically made, because as pointed out by Karato (1993), the temperature derivative of the seismic-wave velocities has an important anelasticity component, which is very sensitive to the *Q*-structure, and realistic calculations ought to consider lateral variations of the *Q*-structure of the upper mantle. As a first approximation based on the presence of amphibole in Kula mantle xenoliths and the stability of amphibole in the upper-mantle conditions, we may place an upper limit of 1050°C on the upper-mantle temperature beneath Kula in western Turkey. In a regional wave propagation study Gök *et al.* (2000) found moderately efficient *Sn* propagation for western Turkey, thereby concluding that the upper mantle in western Turkey is not anomalously hot. Their conclusions are consistent with our estimate of a maximum temperature of 1050°C for the upper mantle in western Turkey.

The spatial and temporal evolution of the extensive Aegean magmatism from the Oligocene to the present can also provide valuable information on the thermal and tectonic history of the lithosphere in western Turkey, along with the *Pn* velocity structure of the region. Gülen (1990) presented a significant positive correlation between the ages of the Aegean calc-alkaline volcanics and granitoids and their relative distances with respect to the Aegean subduction zone. Whereas in the northern Aegean and Marmara regions the ages of the volcanics and granitoids are 25–30 m.y., they become progressively younger toward the active Aegean volcanic arc in the south. Likewise, the upper-mantle *Pn* velocities are high ($\approx$8.0 km/sec) in the north Aegean and Marmara regions, and they become slower toward the south reaching 7.85 km/sec in southwestern Turkey and about 7.6 km/sec in the south-central Aegean sea. If the ages of the calc-alkaline lavas and granitoids are interpreted as indirect indicators of the thermal state of the upper-mantle segment beneath, then the north to south younging trend in the ages of the volcanics may also indicate an upper-mantle temperature gradient increasing in the north–south direction, which would be consistent with the lateral *Pn* velocity variations.

Our results indicate that the upper-mantle *Pn* velocity is 7.85 km/sec beneath southwestern Turkey and increases northward, reaching 8.0 km/sec in the Marmara region of northwestern Turkey. This upper-mantle *Pn* velocity variation is interpreted as due to the thinning of the lithosphere toward the active Aegean arc in the south, where a volatile fluxed, partially melted upper-mantle zone exists just above the northward dipping subduction slab, and the establishment of a consequent upper-mantle temperature gradient decreasing from south to the north. Additionally, the presence of the steeply southward dipping trapped Black Sea oceanic lithosphere beneath the northern Marmara region, as evidenced by seismic tomographic results obtained by Gülen and Kuleli (1995), can also contribute to the advective cooling of the local upper mantle, causing relatively higher *Pn* velocities in the Marmara region.

Conclusions

The seismic velocity structure of the crust in western Turkey is investigated using full-wave synthetic-seismogram modeling. The parameters of the crustal model that satisfy the best-fit synthetic seismograms may be summarized as follows:

The total thickness of the crust is 32 km, and the *Pg* and *Pn* velocites are 5.9 and 8.0 km/sec, respectively, in the Gulf of İzmit, Marmara region. We obtained crustal thickness of 33 km and upper-mantle *Pn* and *Sn* velocities of 7.85 and 4.53 km/sec, respectively, for the Aegean region. A mid-crustal low-velocity zone exists within the crust at a depth of 10–15 km in the Aegean region.

Acknowledgments

We thank Michel Bouchon for valuable suggestions on the discrete wavenumber technique. We thank two anonymous reviewers whose suggestions improved the manuscript significantly. We thank the personnel of the Seismological Laboratory of KOERI for their round-the-clock efforts for data acquisition and processing. Mehmet Yılmazer kindly generated the base map for Figure 1 using the Generic Mapping Tools (GMT) software (Wessel and Smith, 1995).

References

Alptekin, Ö. (1973). Focal mechanisms of earthquakes in western Turkey and their tectonic implications, *Ph.D. Thesis,* New Mexico Institute of Mining and Technology, 189 pp.

Ambraseys, N. (1970). Some characteristic features of the North Anatolian Fault Zone, *Tectonophysics* **9,** 143–165.

Armijo, R., B. Meyer, A. Hubert, and A. A. Barka (1999). Westward propagation of the North Anatolian fault into the northern Aegean: timing and kinematics, *Geology* **27,** 267–270.

Barka, A. A. (1992). The North Anatolian Fault Zone (Spec. issue supplement to v), *Ann. Tectonicae* **VI,** 164–195.

Barka, A. A., and L. Gülen (1988). New constraints on age and total offset of the North Anatolian Fault Zone: implications for tectonics of the eastern Mediterranean region, *Middle East Tech. Univ. J. Pure Appl. Sci.* **21,** 39–63.

Barka, A. A., and K. Kadinsky-Cade (1988). Strike-slip fault geometry in Turkey and its influence on earthquake activity, *Tectonics* **7,** 663–684.

Black, P. R., and L. W. Braile (1982). *Pn* velocity and cooling of the continental lithosphere, *J. Geophys. Res.* **84,** 10,557–10,568.

Bouchon, M. A. (1981). A simple method to calculate Green's functions for elastic layered media, *Bull. Seism. Soc. Am.* **71,** 959–971.

Crampin, S., and S. B. Üçer (1975). The seismicity of the Marmara sea region of Turkey, *Geophys. J. R. Astr. Soc.* **40,** 269–288.

Dewey, J. F., and A. M. C. Şengör (1979). Aegean and surrounding regions: complex multiplate and continuum tectonics in a convergent zone, *Geol. Soc. Am. Bull.* **90,** 84–92.

Erickson, A. J., G. Simmons, and W. B. F. Ryan (1977). Review of heat flow data from the Mediterranean and Aegean seas, in *Structural History of the Mediterranean Basins*, B. J. Duval and L. Montadert (Editors), Editions Technip, Paris, 263–279.

Eyidoğan, H. (1988). Rates of crustal deformation in western Turkey as deduced from major earthquakes, *Tectonophysics* **148,** 83–92.

Fytikas, M. D., and N. P. Kolios (1979). Preliminary heat-flow map of Greece, in *Terrestrial Heat Flow in Europe,* V. Cermak and L. Rybach (Editors), Springer-Verlag, Berlin, 197–205.

Fytikas, M., F. Innocenti, P. Manetti, R. Mazzuoli, A. Peccerillo, and L. Vilari (1984). Tertiary to Quaternary evolution of volkcanism in the Aegean region, in *The Geological Evolution of the Eastern Mediterranean,* J. E. Dixon and A. H. F. Robertson (Editors), *Spec. Publ. Geol. Soc. Lond.* **17,** 687–699.

Gök, R., N. Türkelli, E. Sandvol, D. Seber, and M. Barazangi (2000). Regional wave propagation in Turkey and surrounding regions, *Geophys. Res. Lett.* **27,** 429–432.

Gülen, L. (1990). Isotopic characterization of Aegean magmatism and geodynamic evolution of the Aegean subduction, in *Proc. Int. Earth Sci. Cong. on Aegean Regions*, M. Y. Savaşçin and A. H. Eronat (Editors), Vol. 2, 143–166.

Gülen, L., and H. S. Kuleli (1995). Aegean subduction: a key element in mediterranean tectonics, *EOS, Trans. AGU* **76,** 622–623.

Gülen, L., A. Pınar, D. Kalafat, N. Özel, G. Horasan, M. Yılmazer, and A. M. Işıkara (2002). Surface fault breaks, aftershock distribution, and rupture process of the 17 August 1999 İzmit, Turkey, earthquake, *Bull. Seism. Soc. Am.* **92,** 230–244.

Gürbüz, C., S. B. Üçer, and H. Özdemir (1980). Preliminary results of a seismic experiment in the Adapazari region, Turkey, *Bull. Earthquake Res. Inst.* **31,** 73–88 (in Turkish).

Gürbüz, C., S. Püskülcü, and S.B. Üçer (1992). A study of crustal structure in the Marmara region using earthquake data, in *Multidisciplinary Research on Fault Activity in the Western Part of the North Anatolian Fault Zone,* A. M. Işıkara and Y. Honkura (Editors), Boğaziçi University Publication, 29–41.

Hearn, T. M., and J. F. Ni (1994). *Pn* velocities beneath continental collision zones; the Turkish-Iranian plateau, *Geophys. J. Int.* **117,** 273–283.

Horasan, G., S. Kuleli, and L. Gülen (1996). Crustal structure of the Aegean and Marmara regions, western Turkey, *EOS, Trans. AGU* **77,** 476–477.

Kalafat, D., M. Kara, Z. Öğütçü, and G. Horasan (1992). Determination of crustal structure of western Anatolia, *Deprem Araştırma Bülteni* **70,** 64–89 (in Turkish).

Karato, S. (1993). Importance of anelasticity in the interpretation of seismic tomography, *Geophys. Res. Lett.* **20,** 1623–1626.

Ketin, I. (1969). On the North Anatolian Fault, *Bull. Miner. Res. Explor. Inst.* **72,** 1–28.

Kovachev, S. A., I. P. Kuzin, O. Y. Shoda, and A. L. Solviev (1991). Attenuation of *S*-waves in the lithosphere of the sea of Crete according to OBS observations, *Phys. Earth planet. Inter.* **69,** 101–111.

Kuleli, H. S. (1992). Three dimensional modeling of the Aegean region with seismic tomography, *Ph.D. Thesis* Istanbul Technical University, Istanbul, 107 pp (in Turkish).

Ligdas, C. N., I. G. Main, and R. D. Adams (1990). 3-D structure of the lithosphere in the Aegean region, *Geophys. J. Int.* **102,** 219–229.

McClusky, S., S. S. Balassanian, A. Barka, C. Demir, S. Ergintav, I. Georgiev, O. Gürkan, M. Hamburger, K. Hurst, H. Kahle (2000). Global positioning system constraints on plate kinematics and dynamics in the eastern Mediterranean and Caucasus, *J. Geophys. Res.* **105,** 5695–5719.

McKenzie, D. (1972). Active tectonics of the Mediterranean region, *Geophys. J. R. Astr. Soc.* **30,** 109–185.

McKenzie, D. (1978). Active tectonics of Alpine-Himalayan belt: the Aegean and surrounding regions, *Geophys. J. R. Astr. Soc.* **55,** 217–254.

Mooney, W. D., and L. W. Braile (1989). The seismic structure of the continental crust and upper mantle of North America, in *Geology of North America—An Overview,* A. W. Bally and A. R. Palmer (Editors), Geol. Soc. Am., Boulder, Colorado, 39–52.

Murase, T., and H. Fukuyama (1980). Shear wave velocity in partially molten peridotite at high pressures, Carnegie Inst. Washington Yearbook, Vol. 79, 307–311.

Murase, T., and I. Kushiro (1979). Shear wave velocity in partially molten peridotite at high pressures, Carnegie Inst. Washington Yearbook, Vol. 78, 559–562.

Mysen, B. O., and A. L. Boettcher (1975). Melting of a hydrous mantle: I. Phase relations of natural peridotite at high pressures and temperatures with controlled activities of water, carbon dioxide, and hydrogen, *J. Petrol.* **16,** 520–548.

Panagiotopoulos, D. G., and B. C. Papazachos (1985). Travel times of Pn-waves in the Aegean and surrounding area, *Geophys. J. R. Astr. Soc.* **80,** 165–176.

Papazachos, B. C., P. M. Hatzidimitriou, D. G. Panagiotopoulos, and G. N. Tsokas (1995). Tomography of the crust and upper mantle in southeast Europe, *J. Geophys. Res.* **100,** 12,405–12,422.

Sato, H., S. Sacks, and T. Murase (1989). The use of laboratory velocity data for estimating temperature and partial melt fraction in the low-velocity zone: comparison with heat flow and electrical conductivity studies, *J. Geophys. Res.* **94,** 5689–5704.

Saunders, P., K. Priestley, and T. Taymaz (1998). Variation in the crustal structure beneath western Turkey, *Geophys. J. Int.* **134,** 373–389.

Şengör, A. M. C. (1979). The North Anatolian transform fault: its age, offset and tectonic significance, *J. Geol. Soc. Lond.* **136,** 269–282.

Spakman, W., M. J. R. Wortel, and N. J. Vlaar (1988). The Hellenic subduction zone: a tomographic image and geodynamic implications, *Geophys. Res. Lett.* **15,** 60–63.

Straub, C., H. G. Kahle, and C. Schindler (1997). GPS and geologic estimates of the tectonic activity in the Marmara Sea region, NW Anatolia, *J. Geophys. Res.* **102,** 27,587–27,601.

Taymaz, T. (1996). *S-P* wave travel time residuals from earthquakes and lateral inhomogeneity in the upper mantle beneath the Aegean and the Hellenic Trench near Crete, *Geophys. J. Int.* **127,** 545–558.

Taymaz, T., J. Jackson, and D. McKenzie (1991). Active tectonics of north and central Aegean Sea, *Geophys. J. Int.* **106,** 443–490.

Türkelli, N., D. Kalafat, and O. Gündoğdu (1995). Field observation and focal mechanism solution of November 6, 1992, İzmir (Doğanbey) earthquake, *Jeofizik* **9,** 343–348 (in Turkish).

U.S. Geological Survey (1999). USGS Moment Tensor Solutions, *http://neic.usgs.gov/neis/FM/* (last accessed January 2002).

U.S. Geological Survey (2000). USGS Moment Tensor Solutions, *http://neic.usgs.gov/neis/FM/* (last accessed January 2002).

Wessel, P., and W. H. F. Smith (1995). New version of the generic mapping tools released, *Eos, Trans. AGU* **76,** 329.

Boğaziçi University
Kandilli Observatory and Earthquake Research Institute
81220, Çengelköy
Istanbul, Turkey
(G.H., A.P., D.G., N.Ö., H.S.K., A.M.I.)

GEOSCOPE
57 Edgewater Drive
Framingham, Massachusetts 01702
(L.G.)

Manuscript received 20 August 2000.